

Charge dynamics and recombination kinetics in columnar discotic liquid crystals

Neville Boden, Richard J. Bushby, and J. Clements

Centre for Self-Organising Molecular Systems and the School of Chemistry, The University of Leeds, Leeds, LS2 9JT, United Kingdom

K. Donovan

Queen Mary and Westfield College, University of London, Mile end road, London E1-4NS, United Kingdom

B. Movaghar

Centre for Self-Organising Molecular Systems and the School of Chemistry, The University of Leeds, Leeds, LS2 9JT, United Kingdom

T. Kreouzis

Queen Mary and Westfield College, University of London, Mile end road, London E1-4NS, United Kingdom

(Received 10 November 1997; revised manuscript received 31 March 1998)

The time-dependent quasi-one-dimensional transport of electrons or holes along the molecular columns in columnar liquid crystals has been studied. Recent mobility measurements on the triphenylene-based HAT-*n* materials have revealed Gaussian transits in the liquid crystalline phases but dispersion in the crystalline phases. In this work the factors governing the photoconductivity are rigorously analyzed using random-walk methods. Strong evidence for one dimensionality is found in the time- and electric-field-dependent photocurrent decays. The field begins to affect the decay for values of field energy per hop which are well below kT and comparable with trap concentration as predicted by theory. The trap concentration in the crystalline phase is governed by structural disorder. The traps however appear “shallow” and the long time current disagrees with the deep trap theory. In the liquid crystalline phase, these traps are annealed out by thermal fluctuations and, as consequence, no direct kinetic proof of one-dimensional kinetics is obtainable. This observation of quasi-one-dimensional transport of charge is in keeping with earlier findings for exciton motion in these materials. [S0163-1829(98)04330-6]

I. INTRODUCTION

The charge transport properties of the columnar phases of discotic liquid crystals are not only of fundamental interest, but make these materials potentially useful in applications ranging from sensing devices to high resolution xerography.¹⁻⁶ These properties stem from their unique architecture. They are comprised of disordered stacks of disk-like molecules, such as the hexa-alkoxy-triphenylenes (HAT*n*) arranged on a two-dimensional lattice; see Fig. 1.

The fluctuations in columnar order are sufficient to suppress inhomogeneously distributed structural traps and give rise instead to a uniform “liquidlike” dynamic disorder. As a consequence, the individual molecular columns can transport electronic charge with well defined Gaussian transits.³⁻⁵ Charge carrier mobilities along the columns can be as high as $10^{-2} \text{ cm}^2 \text{ V}^{-1} \text{ s}^{-1}$ and are typically 10^3 greater than in the perpendicular direction. In HAT6 $\mu_{\parallel} \sim 4 \times 10^{-4} \text{ cm}^2 \text{ V}^{-1} \text{ s}^{-1}$ and the intra and intercolumnar distances are $d \sim 3.5 \text{ \AA}$ and $d \sim 19.5 \text{ \AA}$ so that, using $\mu = eD/kT$, we calculate that $D_{\parallel} \sim 10^{-6} \text{ cm}^2/\text{s}$ and $D_{\perp} \sim 10^{-9} \text{ cm}^2/\text{s}$. The latter compares with the value of $10^{-8} \text{ cm}^2/\text{s}$ measured by NMR (Ref. 6) for the molecular self-diffusion coefficient perpendicular to the column axis. Thus the charge carrier transport from column to column is assisted by the occasional molecular hop.

We can therefore expect discotic liquid crystals (DLC's) to exhibit, in a restricted but accessible time domain, truly one-dimensional transport characteristics. In the D_h (self-repairing) mesophase, these materials should be amongst the

best ordered quasi-one-dimensional “transporters” of both charge and excitons.⁷ This is because the liquidlike fluctuations in columnar order which take place on a time scale of less than 10^{-5} s provide an effective self-repairing mechanism. Previous studies of one-dimensional kinetics have been carried out in the pioneering works of Haarer and Moehwald,⁸ Hunt, Bloor, and Movaghar,⁹ Seiferheld, Baessler, and Movaghar¹⁰ for charge transport and by Dlott, Fayer, and Wieting¹¹ and Rughoputh *et al.*¹² for exciton transport.

In this paper, we have to begin by presenting to the reader a number of rigorous mathematical results necessary to understand one-dimensional charge transport in columnar liquid crystalline phases. The theoretical formalism needed to understand the aspect contained in the data cover the dc and ac conductivities. We examine the nature of the stochastic motion in DLC's, the origin of dispersion, the type of disorder, and defects expected. We then present the theory of photoconductivity in the bulk and examine the transient photocurrents with absorbing electrode boundaries in the presence of structural disorder and trapping.

Quasi-one-dimensional systems are exciting because, often, there is new physics to be discovered and it is also the ideal opportunity to verify exact mathematical predictions. This is why so much high quality work has in the past been devoted to studying one-dimensional band structure and dynamics.

Our measurements of carrier transits and photoconductivity are therefore presented with a focus on demonstrating the

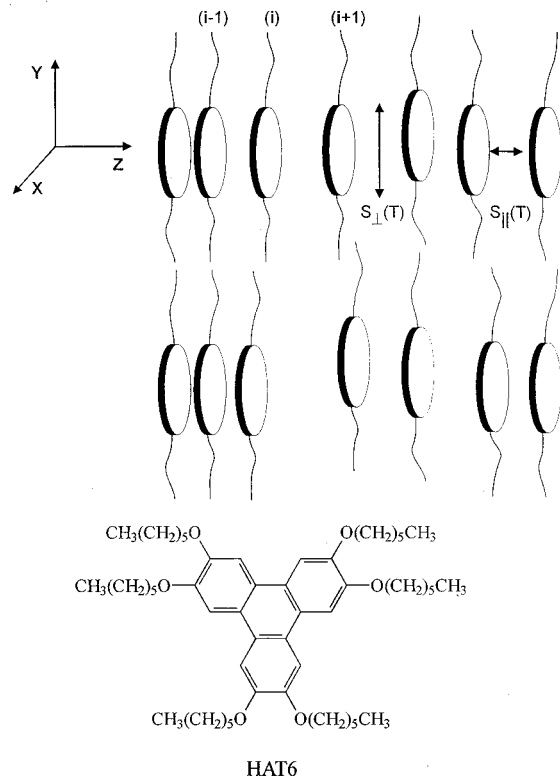


FIG. 1. HAT6: K (67); D (98); I (phase transition temperatures). This figure illustrates a typical discotic liquid crystal HAT6.

existence of one-dimensional (1D) random walk effects. There are a number of rigorous theoretical predictions on photocurrent behavior in 1D which one can use to verify one-dimensionality (see Refs. 8–10). Anomalies which typify 1D behavior are, paradoxically, related to the presence of traps and disorder. In the liquid crystalline phase, unequivocal evidence of one-dimensionality is difficult to obtain. The reason is that in the “liquidlike state” all carriers experience roughly the same trajectory; dimensionality related effects in stochastic transport are however related to quantities which involve deviations from perfect order, such as for example the time to trap,^{8,9} or the drift velocity in the presence of bond disorder.¹⁰ Let us begin by specifying some basic band and transport properties which typify dlc’s. Then later we shall see how to extract the relevant information from the photocurrent data.

II. FACTORS GOVERNING CHARGE TRANSPORT IN COLUMNAR LIQUID CRYSTALS

A. Energy bands

In HAT6, the separation between the molecular cores and columns is ~ 3.5 Å and 20 Å, respectively. There is therefore considerable overlap of π orbitals between the adjacent aromatic rings in a column. The molecules have a highest occupied molecular orbital–lowest unoccupied molecular orbital gap in the range 2–4 eV. Extra charges or excited separated charges have a narrow quantum band structure along the molecular columns with bandwidths $< \sim 0.2$ eV. The resonance energy t_{ij} along the columnar stacks can be written in the usual form

$$t = t_0 e^{-\alpha |R_i - R_j|}, \quad (1)$$

with $\alpha^{-1} \sim 2$ Å and $t_0 \sim 1.0$ eV. This estimate refers to the resonance integral between a charged molecule and a neighboring neutral molecule and the vectors $\{R_i, R_j\}$ refer to the center of the molecular core. When the molecules are tilted with respect to each other, see Fig. 1, then one needs more than one variable to describe the overlap energy. The key quantity in tunneling is the distance of closest approach between the π orbitals.¹³ In the present temperature range (300–400 K) and for the present purposes, it suffices to use the approximate overlap integral given in Eq. (1).

The mobility $\mu_{\parallel}^{e,h}$ parallel to the columns for electrons and holes has been measured as a function of the electric field and temperature.^{3,4,13} Writing

$$\mu_{\parallel} = \frac{eD_{\parallel}}{kT}, \quad (2)$$

$$D_{\parallel} = (l_{in})^2 W_{nn'}, \quad (3)$$

where l_{in} is the average inelastic mean free path. Defining a coherent domain as “ n ,” $W_{nn'}$ is the transition rate between two such domains $\{n, n'\}$ along a column; see Fig. 1.

At zero temperature, we can expect all states in a DLC to be localized and the macroscopic conductivity to vanish. Even in highly ordered samples, the localization length will be short compared to 1D metal, because we are dealing with extremely narrow bands. From the estimates given by Allen,¹⁴ we have roughly $(\alpha\alpha)^{-1} \sim 2(8/\pi)^{1/2} \Delta/2t$, where “ $2t$ ” is half the bandwidth and Δ is the energy disorder width. The polarization fluctuation width is at least ~ 0.01 eV and “ t ” is at most ~ 0.2 eV in the HAT n , so the localization length is at most ~ 14 lattice constants. In the pure stochastic limit, $l_{in} \equiv a_{\parallel}$, and at room temperature and above, we can consider the transport along the columns to be essentially stochastic or diffusive with a coherence length l_{in} which is $\geq a_{\parallel}$.

B. Defects and traps

In a columnar liquid crystal, one can expect the following types of defect: (a) chemical impurities which lead to the trapping of charge; (b) structural defects, such as large amplitude displacements of molecules which can also be produced thermally, and can therefore also self-repair (see Fig. 1).

In undoped materials, there are very few ionized chemical impurities ($< 10^{10}$ cm³) at room temperature. The number of impurities which can act as traps for free charges is of course well in excess of that number.

Most of the charged chemical defects will be due to reaction with the metal electrodes. Most defects in general are structural and can self-repair. This is the reason why one can have well defined, Gaussian transients in an otherwise, highly unfavorable topological situation. The density of the structural traps can be estimated as follows: if V_0 is a typical energy required to generate a substantial break in a column, $0.3 < V_0 < 1.0$ eV, then the coherence length in one dimension is given by

$$\xi(T) \sim a_{\parallel} e^{V_0/2kT}. \quad (4)$$

At $T=300$ K and in a strictly one-dimensional approximation, $\xi(T)\sim 10^{-7}-10^{-4}$ cm. The time to create or repair such a defect is known from NMR linewidth and anisotropy measurements. In the D_h phase of HAT5, $\tau_d\sim 10^{-5}$ to 10^{-6} s. We expect $\tau_d(T)$ to decrease with increasing side chain length. *The melting temperature $T_m(n)$ is a decreasing function of n as shown in Table 1 of Ref. 15.*

A typical electron or hole transit across a distance d takes a time τ_T given by

$$\tau_T\sim\frac{d}{\mu F}. \quad (5)$$

With $d\sim 10^{-3}$ cm, $\mu\sim 10^{-4}$ cm² V⁻¹ s⁻¹, and $F\sim 10^4$ V cm⁻¹, $\tau_T\sim 10^{-3}$ s, so that $\tau_T\gg\tau_d$ in the D_h phase. The main scattering event for a carrier moving in a column therefore consists of a combination of displacements as shown in Fig. 1. In the crystalline phase, sideways structural displacements are ‘‘permanent’’ on the time scale of a transit and therefore give rise to real long-time traps or barriers with a distribution of energy $P_n(\epsilon_v)$ which depends on the side chain length. In the liquid crystalline D_h phase, the structural traps self-anneal so that carriers do not suffer any long term trapping.

To quantitatively characterize a given material, a mathematical model of the transport process is required. The model can then be compared with experiment from which we can extract the parameters which measure the degree of disorder.

In quasi-three-dimensions, the disorder is contained in the quantities $W_{\parallel}(p)$ and $W_{\perp}(p)$ which characterize the effective frequency dependent jump rates in the two main directions along and perpendicular to the columns. The ac conductivities ($p=i\omega$) then become^{16,17}

$$\sigma_{\parallel}=\frac{n_c e^2}{kT} a_{\parallel}^2 W_{\parallel}(i\omega), \quad (6)$$

$$\sigma_{\perp}=\frac{n_c e^2}{kT} a_{\perp}^2 W_{\perp}(i\omega), \quad (7)$$

which can always be represented to a good approximation by a semiempirical scaling law which includes anisotropy, the dc limit ‘‘ p_{dc} ,’’ high frequency saturation at ‘‘ ν_1 ,’’ and the effect of the ordered domain length ‘‘ l_c ,’’ (aggregate coherence size) would be

$$D(p)=[(l_c^2)/2][p_{dc}][1+\{(p_1/p_{dc})\}^s], \quad (8)$$

$$p_1=p\nu_1/(p+\nu_1). \quad (9)$$

The time-dependent diffusion in strictly 1D systems with disorder is however highly anomalous as shown rigorously in Ref. 17. The time-dependent part of the drift becomes sublinear with applied field and linear response theory breaks down. We shall come back to this point later in the text in Sec. III C. The present class of materials is in some respects ideal to verify such predictions.

C. The influence of inhomogeneities:

Trapping versus dynamic disorder

The scaling laws of type 13 apply to uniform disorder models. Experiment shows that the crystalline state cannot be characterized by uniform disorder only. There is disorder caused by misalignment, grain boundaries, and polycrystallinity.

The effect is to make the ac conductivity frequency dependent where it should in principle still be constant. This type of disorder causes structural traps and has to be treated differently than homogeneous disorder. There are various ways we can model this kind of disorder. One can allow a trapping contribution to the random walk as shown in Ref. 18. The simplest way is to allow a particular group of molecules to be locally frozen into configurations of the type shown in Fig. 1. This causes a larger than normal Gaussian broadening for the molecular displacements from equilibrium and, consequently, a larger local resistance. One can treat such situations exactly but, in order to simplify the algebra, we assume that processes which give rise to trapping^{18,19} return to the transport path, and molecular rotations and motions, i.e., all events which delay the carrier, can be treated using a single delay time function:

$$m_i(p)=p\langle\sum_j\{W_{ij}/(W_{ji}+p)\}\rangle \quad (10)$$

such that we now simply have to replace the frequency p with $\{p+m(p)\}$ and carry out the configuration average over all possible delay processes that the carriers encounter in the crystalline phase. The average introduces an order parameter $h(T)$ which goes to ‘‘0’’ or strongly decreases when the system enters the D phase.²⁰ We can write $m(p)=h(T)\Psi(p)$, where $h(T)=[\{T_D-T\}/T_D]^s$. This waiting time function enhances the dispersion and gives a lower effective static diffusivity. Naturally we can give the configuration shown in Fig. 1 a mathematically rigorous treatment if necessary: allow both bonds to be distorted and also include rigorously the change in the inter and intracolumnar jump process. The delay time function procedure is however elegant and in some way more general since it allows classical as well as quantum processes to be integrated into a single function with a universal shape. See Appendix A and the work of Scher and Lax.¹⁸

Using the universal ac structure (8) we now have, for the diffusivity, the form

$$D(p)=\{1/(1+h(T)\Psi(p))\}D\{p[1+h(T)\Psi(p)]\}, \quad (11)$$

where we simply replace the frequency variable ‘‘ p ,’’ with $\{p+m(p)\}$ and multiply the diffusivity by $p/(p+m(p))$. If the trap free diffusivity was frequency independent, then the effect of the traps is only due to the latter factor. Finally, this factor has to be squared, if we do not count the traps as part of the diffusion sites where the particle can be found.

This analysis now allows different kinds of disorder processes: dynamic and static ones which can be integrated into a single function. Depending on purity, and speed and nature of the dynamics, a given discotic material might exhibit transits while another will show pure dispersion. The diffusivity (11) is plotted in Fig. 2 for three different values of trap density, using the waiting time function $\Psi(p)$

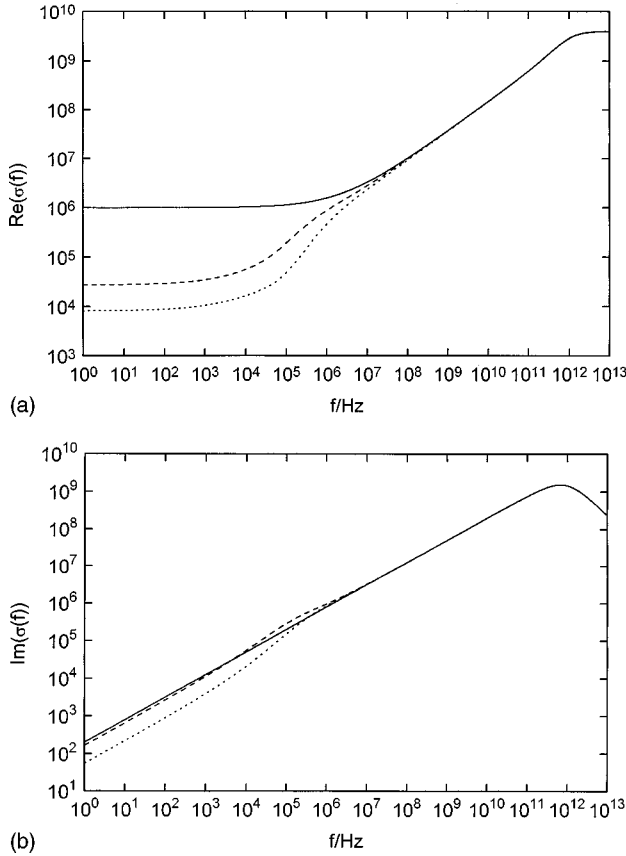


FIG. 2. Plot of the theoretical diffusivity $\text{Re}\{D(i\omega)\}$ vs ω obtained from Eq. (11), illustrating the change that occurs when the system goes from the state of Gaussian overlap disorder (D_h phase) to the situation where in addition we now also have structural traps with long delay times (crystalline phase). The upper curve: $N = 0$; middle: $N = 5$; lower: $N = 10$; N = equally accessible non-transporting trapping sites per molecule.

$=N_1\{1+(p/\nu_i)^{\kappa}\}^{-1}$. The figure clearly illustrates the difference between the homogeneous disorder case and the case when the carrier encounters the occasional deep trap caused by serious structural deformations as in the polycrystalline state of HAT and most discotic liquid crystals. The diffusivity is needed to evaluate the photocurrent transits.

III. THEORETICAL BACKGROUND FOR UNDERSTANDING PHOTOCURRENTS IN DLC'S

A. The time decay of the bulk photocurrent

The photocurrent I_p contains information on the distribution of traps in a nonequilibrium situation, the influence of boundaries as in a transit experiment^{3,4} and also on the dimensionality of the carrier motion and dimensionality cross-over with time (t) and temperature (T). Consider the bulk photocurrent in the absence of absorbing boundaries, with an effective time-dependent mobility $\mu(t)$ or diffusivity $D(t)$

$$\mu(t) = \frac{eD(t)}{kT} \quad (12)$$

and a carrier survival fraction $n(t)$. The carriers can be delayed by structural traps. They can however also fall into deep traps from which they do not escape during transit (re-

combination centers). Assuming these centers do not allow escape, then we can discuss this situation in the context of deep trap models.

First we have

$$I_p(t) = G\tau_\phi \frac{eF}{kT} n(t)D(t), \quad (13)$$

where G and τ_ϕ are the generation rate and laser pulse length, respectively, from which it follows that for constant diffusivity $D(t)$, the time dependence of $I_p(t)$ is entirely due to the survival fraction $n(t)$. The latter can be evaluated exactly as a function of $W^\pm(p)$, the effective with (+) and against (−) field jump rates. For most situations of interest, the density of recombination centers is low so that carrier diffusion to those centers can be assumed to take place in the steady state. In general,^{16,17,21,22} for experimental times $t > \tau_\phi$, the pulse time, and free carrier generation time, we have

$$D(t) = D_0(t) + \frac{D_1}{t^\beta}, \quad 0 < \beta < 1 \quad (14)$$

where the time dependence covers the region up to the critical hop frequency.^{16,17} Assuming here that $D(t) \sim D_0$, a constant for all times, we can write to a good approximation

$$n(t) \approx n_{\parallel}(t)n_{\perp}(t), \quad (15)$$

where n_{\perp} is the survival probability due exclusively to diffusive motion in the anisotropic network (when $\eta < x$) (Refs. 17 and 23) (the case $\eta > x$ is given in Appendix B)

$$\begin{aligned} n_{\parallel}(t) = & \frac{4}{\pi^2} e^{-\eta^2 D t / a^2} \int_0^\infty dS \frac{S}{[1 + (\eta S / \pi x)^2]^2} e^{-\pi^2 x^2 (D t / a^2 S^2)} \\ & \times \left[\frac{e^{-S}}{1 - e^{-S}} + \frac{e^{-S(1 - \eta/x)}}{2(1 + e^{-S(1 - \eta/x)})} \right. \\ & \left. + \frac{e^{-S(1 + \eta/x)}}{2(1 + e^{-S(1 + \eta/x)})} \right] \end{aligned} \quad (16)$$

and

$$n_{\perp} = \exp[-xct\{D_{\parallel}D_{\perp}\}^{1/2}/(a_{\parallel}^2 + a_{\perp}^2)] \quad (17)$$

is the first passage time (FPT) (Ref. 17) result. Here x is the concentration of deep traps; c a constant ~ 1 . For a strictly one-dimensional random walk $D_{\perp} \equiv 0$, and we have the exact one-dimensional result which has a very characteristic time and electric-field scaling behavior as discussed in Ref. 22. The term (17) is a way of taking into account approximately the trapping events caused by the sideways walks of the particle when it moves on the anisotropic network. The combination (15) of course somewhat overcounts the trapping events but the reader should note that the term (17) only manifests itself in the long time limit and at low fields, then it controls the decay.

Here we note that a strictly one-dimensional walk gives rise to the long time law

$$n_{1D}(t)_{t \rightarrow \infty} \sim e^{-3[(\pi^2 x^2 t / 4a^2) D]^{1/3}} \times 16 \left(\frac{x^2 t D}{3\pi a^2} \right)^{1/2}, \quad (18)$$

when $\eta < x$. When $\eta > x$ the recombination is drift limited and a simple exponential is given by Eq. (A2) in the Appendix.

By using the information we have from dc and ac conductivity, we can determine x and the dimensionality crossover from a detailed study of the photocurrent. Clearly the D_h phase is the ideal phase in which to study x since here we can distinguish shallow from deep traps. The former determine $D_0(T)$; the latter the long time decay of $I_p(t)$.

The two factors in Eq. (15) describe one-dimensional (exact) and anisotropic three-dimensional transport in the framework of the first passage time method. Equation (15) describes the competition between three-dimensional and one-dimensional motion. Three dimensionality dominates at long times in low fields.

B. The theory of photoconductive transits: The influence of an absorbing boundary

Now we consider transient mobility experiments and show how one can calculate the experimental photocurrent knowing the frequency dependent diffusivity $D(p)$. We introduce an absorbing boundary at L and using the derivation in Refs. 23 and 24 we arrive at the following form for the Laplace transformed photocurrent:

$$I_p(p) = \int_0^\infty e^{-pt} I_p(t) dt, \quad (19)$$

$$I(p_1)/N_c = (eF/kT)D(p_1)/p_1 \times [1 - \exp\{-Np_1/(p_1 + 2\eta D(p_1)/a^2)\}], \quad (20)$$

where $N = L/a$, and the quantity $1/p_1$ is given by the Laplace transform of the survival fraction $n(t)$ also referred to as $n(p)$; when recombination has no time to intervene, we can replace $p_1 = p$; for details of how to calculate $n(p)$ see Ref. 23. The replacement $1/p$ with $n(p)$ is basically saying that the transport process can be cut off by the deep trapping events. The factor in the square bracket is the effect of the boundary. The initial light generated free carrier density is N_c . This number depends on the details of the light induced generation process near the electrode boundary of the liquid crystal/metal contact. For HAT- n the penetration depth of the $\lambda = 335$ nm light is $\sim 0.1 \mu\text{m}$.

The frequency dependence of $D(p)$ in Eq. (20) is typically as shown in Fig. 2 for the K and D phase.²⁵ Measurements of $D(p)$ using ac conduction in undoped samples are difficult to interpret because electrode polarization effects and ionic contributions mask the weaker dispersion along the columns.

C. The time dependence of the transient photocurrent $I(t)$: analytical results

Equation (20) can be numerically inverted and allows a frequency dependent jump rate. Analytical results can be found in several limits. In order to obtain the time dependence of Eq. (20), we consider several limiting cases.

(a) Dispersion parameters “ α ” = 0, $D(p) = D_0$, and trap concentration $x = 0$. Here we have, in the limit that back diffusion can be neglected [$v_d = 2\eta D/a$, $N = L/a$],

$$I(t, x=0) = \{eFN_c/kT\}D_0(T)\exp[-tv_d/L] \times \left\{ \sum_{n=0}^N (v_d t/L)^n/n! \right\} \quad (21)$$

or to a good approximation with back diffusion

$$I(t, x=0) = (eN_c)d/dt \left\{ \int_0^L dy (4\pi Dt)^{-1/2} y \times \exp[-(y - \mu Ft)^2/4Dt] \right\}. \quad (22)$$

This formula assumes that the boundary does not influence the propagator while the carrier is still on its way and represents therefore a slightly more classical picture, which is indeed probably more appropriate to liquid crystals than the exact semiclassical random-walk result. Within our present measurement accuracy, the difference between Eqs. (21) and (22) is however insignificant. The same applies to the exact formula which includes both back diffusion and boundary effects and which is given in Ref. 17 and in the Appendix of Ref. 23 in Laplace space. Deviations from Eq. (22) should be insignificant in the present time regime.

(b) Now let us allow a finite $x > 0$; this introduces a survival fraction $n(t)$ so that

$$I(t) = I(t; x=0)n(t). \quad (23)$$

The boundary gives rise to a fast decay of the surviving carriers which get there.

(c) The dispersion parameter is $\alpha = 1/2$, and x is finite:

$$I_t(t) = (eFN_c/kT)(D_1/t^{1/2})[1 - \exp\{-t_T/t\}]n(t), \quad (24)$$

$$v(t) \sim eF/kTD_1/t^{1/2}; \quad (25)$$

the time of transit is defined by the time taken to reach the boundary ($2\eta = eFa/kT$)

$$\int_0^{t_T} dt' v_d(t') = L; \quad t_T = [L/4\eta D_1]^2. \quad (26)$$

In this formula it is assumed that $D(t)$ is still time dependent on the scale of the transit time defined above; strictly speaking $n(t)$ must now also be evaluated using a time-dependent diffusivity. We do not have an exact analytical formula for this situation. It is however reasonable to suppose that one can replace Dt with $\int_0^t dt' D(t')$ in Eq. (16). A better way is to use the FPT method instead and write

$$n(t) = n(o)\exp[-x(t/t_0)^\gamma]. \quad (27)$$

This then treats γ as the time exponent of the number of new sites visited^{24,26} and accounts for dispersion, electric field, dimensionality, and temperature. If $D(t)$ or more precisely $v_d(t)$ reaches the steady state value before the boundary (weak dispersion) then (a) applies in the long time limit and $n(t)$ can be computed using the exact formula (16).

(d) Same as (c) but with a general dispersion parameter “ α ” and finite trap concentration x :

$$I_t(t, x) = \{eFN_c/kT\}D_0(T)n(t)\{D_1/t^\alpha\} \\ \times [1 - \exp\{-(t_T/t)^{2(1-\alpha)}\}], \quad (28)$$

$$t_T = \{L(1-\alpha)/2\eta D_1\}^{(1/1-\alpha)}. \quad (29)$$

giving, assuming linear response to apply (see note below),

$$(i) \quad I_t(t) \sim eFa/kTn(t)1/t^\alpha \quad \text{for } v_d t \ll L, \quad (30)$$

$$(ii) \quad I_t(t) \sim F^{(2\alpha-1)}n(t)1/t^{\alpha}1/t^{2(1-\alpha)} \quad \text{for } v_d t \gg L, \quad (31)$$

with $n(t)$ given by the FPT formula (27). If we put $\alpha = 1 - k$, we have the characteristic Scher-Montroll dispersive transit law.²⁷

Comment

Note that the factor $n(t)$ only intervenes if the carrier has a good chance to be trapped before reaching the electrode, i.e., when $x > (a/L)$. Since Eq. (31) assumes that the drift is dispersive for long times compared to the transit, the correct survival fraction in the presence of dispersion would be the FPT form given by Eq. (27) rather than the exact $n(t)$ given by Eq. (16).

Note that N_c is the number of photocarriers escaping recombination in the generation zone. This quantity also depends on T and F and determines the magnitude of the signal.

Note. In strictly 1D with dispersion, the drift velocity was shown rigorously to be sublinear with field^{21(b),22} as long as the drift is still time dependent. Linear response is no longer valid in the time-dependent regime and this would have consequences on the behavior of Eq. (26) since we have

$$v_d(t) \sim 2\eta D_2 / (\eta v_0 t)^\alpha \quad (\text{one-dimensional transport}). \quad (32)$$

The sublinearity with field simply means that the drift in one direction is also enhancing the number of new sites (bonds) visited and therefore also the probability of encountering a worse hop which slows down the carrier. Normality or linear response is only recovered when the carrier has encountered the worst situation on its way to the electrode. The anomalous field dependence has consequences for the field dependence of the transit time evaluated for example in Eq. (26) where it was assumed that the drift is linear in field in the dispersive regime.

Now that we have given the reader the necessary tools for interpreting mobilities and photocurrents in quasi-one-dimensional systems, let us consider the experimental results obtained for HAT6.

IV. EXPERIMENTAL METHODS

A. Transient photocurrent measurements

In order to measure the hole mobility in the mesophase of the HAT6 technique due to Kepler and Leblanc, time of flight transit was employed. In this technique, the sample is contained between two electrodes separated by d , in this case

defined by a 20 μm mylar spacer. One of these electrodes is semitransparent and, further, the skin depth for absorption of the light used to excite carriers (337 nm from a 6 ns nitrogen laser pulse) is less than one micron. A pulse of light incident on the semitransparent electrode immediately creates carrier pairs in the material, one sign of which is swept out immediately at the semitransparent electrode while the remaining sign of carriers drifts towards the counter electrode. Upon arrival at the counter electrode, the current will fall rapidly as the carriers discharge. The current is measured as a voltage drop across a load resistor whose magnitude is chosen to reflect the time response required for the particular experiment always keeping RC_s less than the transit time where C_s is the sample capacitance. Thus

$$RC_s \ll T_{Tr} = d^2/\mu V, \quad (33)$$

where μ is the mobility of the carrier. A variety of preamplifiers have been used where necessary again ensuring that the time does not affect the measurement.

In the case of HAT6 transits are observed only from holes in the mesophase and featureless decays are observed for electrons and from holes in the crystalline phases. These are due to trapping/recombination of the carriers before arrival at the counter electrode. Such decays are however fitted to determine other transport properties concerned with the trapping/recombination. To carry out such fitting the signals are captured using a digitizing oscilloscope and subsequently analyzed. The asymmetry concerning electrons and holes is due to the fact that in the present materials there are many more electron traps (O_2 and oxidation products) than hole traps.

In taking measurements great care was taken to avoid two possible problems.

(i) Where there is carrier trapping (crystalline phase for holes and all phases for electrons) it is essential to apply the electric field and take the measurements immediately. The field is then reduced to zero while pulsing the light. This ensures that there is no buildup of trapped charge in the sample acting to distort the electric field. It is found that if this procedure is not followed the measured signal rapidly reduces to zero after a few pulses.

(ii) It is necessary to ensure that there are no space charge distortions of the electric field due to the transiting unipolar charge. This involves keeping the light intensity down such that the photocharge is always at least a factor 100 below the space charge limit. From the measurement of the peak photocurrent in the current decay regimes the mobility may be found in the absence of transits provided the total charge created is known, using

$$I = q\mu E/d. \quad (34)$$

B. Comparison theory experiment: Analysis of transient photocurrents in the “ordered” liquid crystalline phases

Looking for proof that the motion is quasi-one-dimensional is not a trivial task. The theoretical formalism developed in the previous section for the transit current tells us that dimensionality of the transport can actually only be seen in the trapping function or in the anomalous drift term. Both imply disorder in some form. A regular random walk

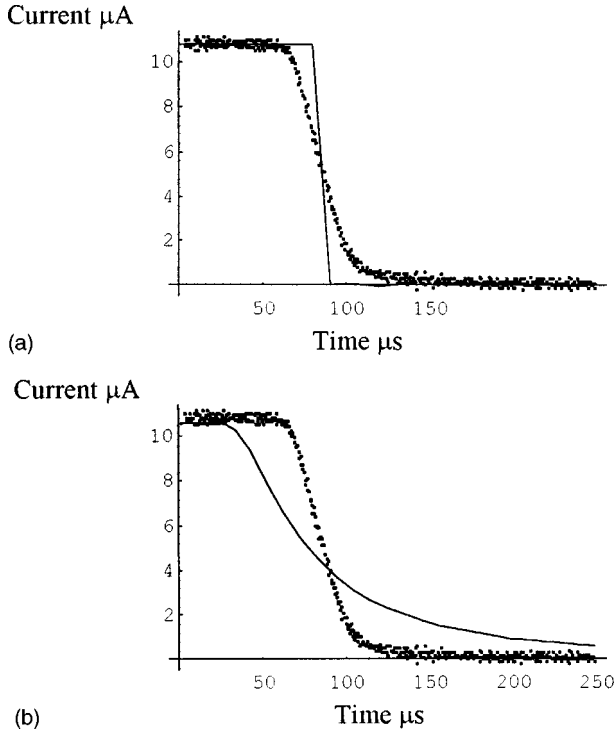


FIG. 3. (a) The photocurrent transit in the D_h phase of HAT6 at a field of 5 MV/m; the solid curve is the theory given by Eq. (16) and which assumes no dispersion at all. This accounts for the somewhat too rapid decay at arrival. (b) A comparison with Eq. (28) strictly applicable only to dispersive transport (Scher and Montroll limit) in the limit of weak dispersion ($\alpha \sim 0$).

has no special characteristics even in the presence of weak dispersion. The information on dimensionality in the liquid crystal phase must therefore be sought in the decay curves at long times or in the sublinear electric field dependence of the drift velocity as was shown in the previous section (III). Here in this section we verify the existence of a remarkably well behaved transit by looking at Figs. 3(a) and 3(b). As shown in Fig. 3(a), the fit to the formulas (21) and (22) which assume direct drift into the boundary is far superior than to the dispersive law (28) in the limit of weak dispersion; Fig. 3(b). Allowing regular drift and diffusion into a region which becomes disordered only near the absorbing boundary would, we believe, give the best possible model. This will be considered in a future paper. This dramatic change in going from the C to the D phase in the HAT's is connected with the rapid self-annealing of structural traps as illustrated by the change in the ac conductivity shown in Fig. 2.

C. Analysis of the photocurrent decay in the disordered crystalline state

Consider now the crystalline state. The photocurrent is strongly dispersive so we do not see a well defined knee in the transit curves.

Figures 4(a)–4(c) are a plot of $I_p(t)$ versus time using Eq. (16) to fit the experimental data (solid lines are theory) for the following parameters: $F=1.5$ MV/m; 2.5 MV/m; 5 MV/m, $T=300$ K, $W=1.2 \times 10^{10}$ Hz. Fit values of trap concentration are $x=$ (a) 0.0014, (b) 0.0011, and (c) 0.001, respectively. This corresponds to a value of mobility

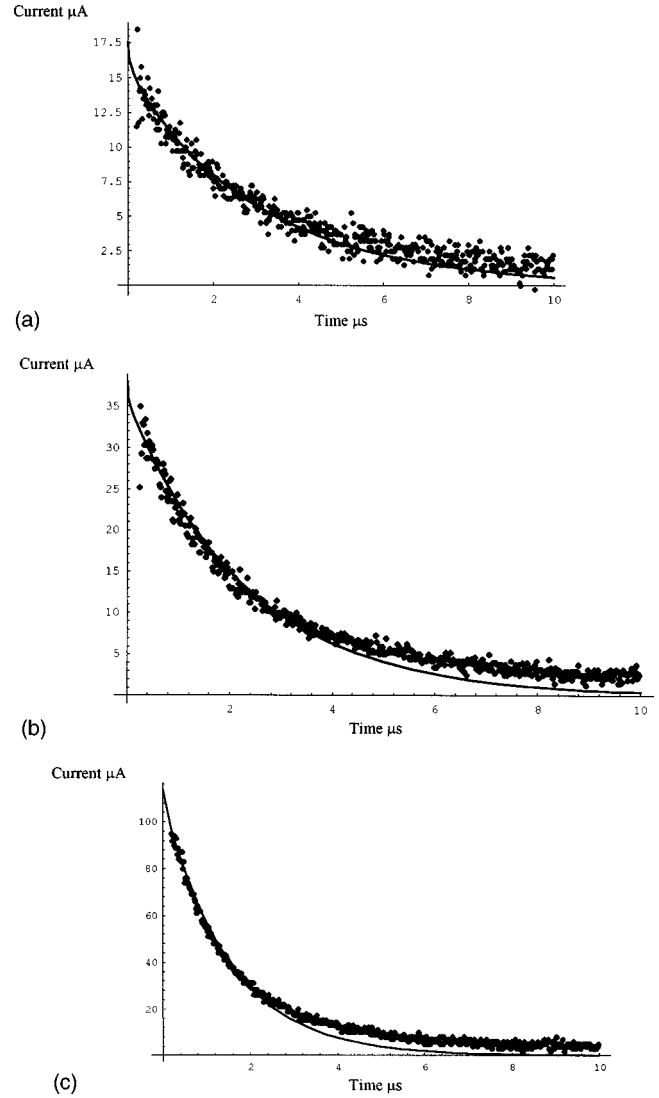


FIG. 4. The time decay of the pulsed transient photocurrent of HAT-6 in the crystalline phase: a comparison of experiment to theory (solid line). The best parameters are for $T=300$ K. (a) 1.5 MV/m, $W=1.2 \times 10^{10}$ s, and $x=0.00027$; (b) 2.5 MV/m, $W=1.2 \times 10^{10}$ s, and $x=0.00022$; (c) 5 MV/m, 1.2×10^{10} s, and $x=0.00015$. Figure 3(b) illustrates the strong dependence of the time decay on the field: a signature of low dimensional transport.

$$\mu_{\parallel} = \frac{eD_{\parallel}}{kT} = 3 \times 10^{-4} \text{ cm}^2 \text{ V}^{-1} \text{ s}^{-1}. \quad (35)$$

The crossover from one-dimensional to three-dimensional motion should take place when

$$xt(D_{\parallel}D_{\perp})^{1/2}\{a_{\parallel}^2 + a_{\perp}^2\}^{-1} \sim 1. \quad (36)$$

This defines the time windows $t < t_c$ and $t > t_c$. The crossover from diffusion to drift limited recombination takes place when $\{eFa_{\parallel}/kT > 2x\}$.

The photocurrent decay in a crystal as a function of field with a relatively large number of traps is an ideal situation in principle to verify the 1D kinetic laws as predicted by Eq. (16). Excellent agreement is found between 1D theory and experiment with a consistent trap density of $x \sim 10^{-3}$. Agreement is better at low fields than at high fields when looking

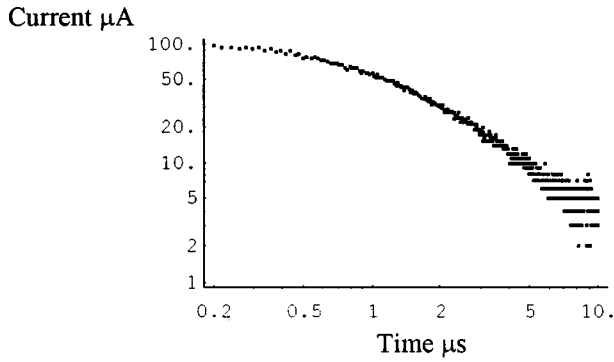
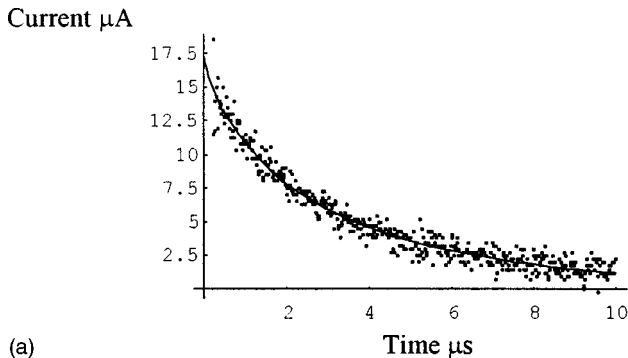
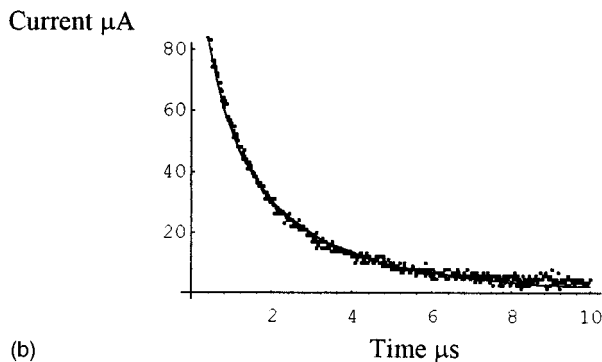


FIG. 5. Log-log plot of the crystalline photocurrent transient of HAT6 for $F=5$ MV/m under (c) in Fig. 2. Note that one cannot identify a genuine knee in the transit plot at all.

at long times. This is a strong indication that traps are not infinitely deep on the experimental long-time scale and that some carriers can detrapp with field and temperature and reach the electrodes. Figure 5 shows that even the 1D law is somewhat too fast at long times. The log-log plot of photocurrent does not however exhibit a convincing transit knee as can be seen in Fig. 6. At the largest fields measured, the decay in the crystalline phase obeys a simple exponential law at long times with a time constant which is given by $\sim 1/xv_d$ as predicted by the exact 1D formula (B2) in Appendix B.



(a)



(b)

FIG. 6. The transient photocurrent decay of HAT6 in the crystalline phase is plotted against the FPT type laws “ $\exp[-xbt^\gamma]$ ” for $F=1.5$, MV/m, $\gamma=0.75$ and for $F=0.5$ MV/m $\gamma=0.61$. The exponent γ is a measure of dimensionality and within FPT would be 0.5 for a perfect 1D walk. The variation of γ with the field is probably of no great significance; the increase of b with the field however is, and signifies that we are not dealing with a two or three-dimensional random walk, since this would not give a detectable field dependence in this range.

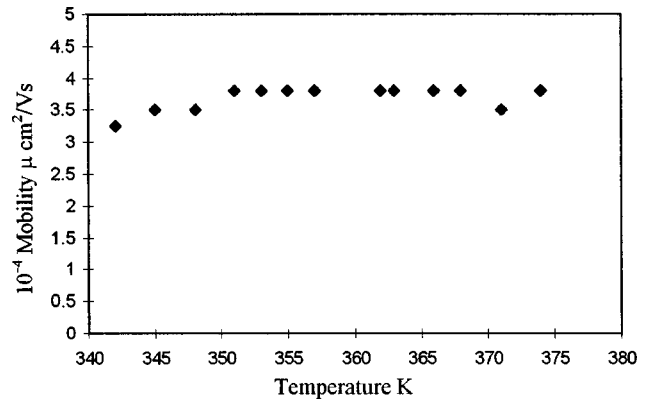


FIG. 7. Plot of the measured mobility $\mu(T)$ of HAT6 in the D_h phase versus temperature T .

To account for the constant long time photocurrent, we would need to allow for more complex considerations such as detrapping processes or electrode polarization. This will be discussed in a future paper.

D. Can we observe dimensionality crossover laws?

We are in reality dealing with a transport process which is not purely one-dimensional. We might be able therefore to detect at later times a crossover from a one-dimensional to a three-dimensional random walk. Given the fact that temperature decreases the anisotropy ratio (W_\perp/W_\parallel), and the fact that the one-dimensional to three-dimensional behavior changes the exact asymptotic $e^{-t^{1/3}}$ law into an e^{-t/t_0} law, we might therefore expect to see a fit to a scaling law of the form

$$I_p(t) = I_p(0) e^{-(t/t_0)^{\gamma(T)}}. \quad (37)$$

The exponent $\gamma(T)$ depends on temperature, the anisotropy of the material, and the time regime. We expect $\gamma(T) \sim 1/3$ in the crystalline and discotic phases and then crossover $\gamma \rightarrow 1$ as $T \rightarrow T_c$. The change from $\gamma < 1$ to $\gamma = 1$ should be clearly visible at the D to I phase transition in the time window $0 < t < t_c$. Figures 7(a) and 7(b) show a comparison between experiment and Eq. (28); the experimental behavior is not as expected from this discussion. Equation (27) can be made to fit the data, with a value of $\gamma \sim 0.6$ with little variation. This would normally signify a “two- to three-dimensional” kinetics, but the fact that the electric field dependence of the decay function comes earlier than expected for such a dimensionality ($d > 2$) suggests that the fit though obviously good is probably of no great physical significance because, in the absence of boundary effects and space charge effects, the principle mechanism for field-dependent decay at small fields ($\eta < kT$) is one dimensionality of carrier motion so that the exact 1D law is very likely the better representation. This at least appears to be so for the short and intermediate time domains. The very long time decay in the domain $eF/2kT \gg x$ is purely exponential as predicted by Eq. (B2) and “the almost constant value of I_p ” is consistent with shallow traps. In this case we should expect a “transit” when the steady state long time current reaches the boundary; this will be studied in a future experiment. Long time very weakly decaying photocurrents are however very com-

mon in organic materials and also in smectic liquid crystals.²⁸ They could be due to polarization changes in the medium, especially at the boundary of the electrodes. The dielectric changes induced by the light pulse causes a lowering or change in the electronic barrier between metal and organic and this gives an increase in the current which can take a very long time to decay.

E. Discussion: The temperature dependence of the carrier mobility and the role of phase transitions

The measured mobility in the D_h versus temperature is shown in Fig. 7. We did not measure μ in the other phases of HAT6. The photocurrent in the isotropic phase was too small. In the K phase, it is too dispersive.

We know however from charge injection and resistivity measurements on HAT6 (Ref. 6) that the phase transitions C (70) to D (100) to I affect the mobility.^{4,5} Theoretically, the mobility in each phase can in principle be calculated from first principles, provided we know the distribution function of the molecular positions. The distribution can only be defined to the phases, not to the phase transitions. In strictly 1D, we can also use exact results for the conductivity if necessary. For practical purposes, in analyzing the data, it is useful to attempt to give a semiempirical relationship. Knowing that when disorder sets in, it is resistances that add, one might write

$$1/D(T) = [1 - G(T)]S(T)/D_{\parallel} + G(T)[1 - S(T)]/D_I, \quad (38)$$

where $S(T)$ is the short range order parameter, $D_{\parallel, I}$ are the diffusivities along the column and in the isotropic phase, and $G(T)$ is a geometric weighting factor which gives us a measure of the number of broken columns or aggregate lengths. The combination G and S in Eq. (38) can also be considered to be the effective transport order parameter measuring the number of *normal* (along the column) and *anomalous* (perpendicular or at a defect) hop processes. Since $D(T, \omega)$ and $S(T)$ can be measured in all three phases, the latter by optical methods for example,²⁵ we can estimate the number of ‘‘normal’’ and ‘‘anomalous’’ jumps that the carrier performs on its way to the electrode, at a given temperature, using Eq. (38). Comparison to experiments in discotic materials where such data exist^{3(b),18} suggests remarkably that, with Eq. (38), the break in the order must be extremely sharp with $s(T)$ undergoing a very abrupt change from ‘‘1 to 0.’’ In terms of μ in Eq. (16), it implies a value close to ‘‘0’’ (~ 0.05). The apparent sharpness of the conductivity requires some further discussion.

In quasi-one-dimensional systems, simple averages of sums can be misleading because the fluctuations are not necessarily on an intermolecular scale only⁴ and such systems are not always self-averaging on the experimental length scale. It might be better under certain circumstances (ideal interface and order) to average the ‘‘resistance’’ logarithmically.²⁹ In this case the transition will be sharper and in the exponent of the conductance rather than in the conductance itself, with the transition from normal to anomalous hops with

$$W^{-1} \sim \exp[2\alpha R_{\text{opt}}], \quad (39)$$

where R_{opt} has to be evaluated with a model distribution of disorder²⁹ and will undergo a sharp transition at the clearing temperature (D to I). At the phase transition all molecular coordinates change simultaneously and give rise to a new average molecular separation so that we have $R_{\text{opt}} = R_{\parallel}[1 - s(T)] + R_I s(T)$.

These subtle differences that may exist between ways of averaging disorder when we are far from phase transitions depend very much on sample quality and width of the measuring cell. We have not been able to observe a photocurrent transit in the I or C phases of HAT- n at all. Adam *et al.*,³ however, have measured the mobility in all three phases (glass at low T) of related materials (HHTT and HPAT2); the mobility changes seen by these authors can be described by Eq. (38) only if the order parameter changes abruptly at the phase transition, i.e., has a smaller exponent than the ones measured by Phillips and Jones on discotic nematic mixtures.²⁵ This is to be expected for a pure discotic liquid crystal. Interestingly it also allows us to conclude that the pretransitional large amplitude thermal fluctuations which must occur in the liquid crystal phase of HAT- n , and which would support a smoother transition in mobility, are indeed self-repairing on a time scale which does not appear to seriously slow down the carriers. This is a remarkable phenomenon indeed.

Adam, Rohmildt, and Haarer¹⁹ have measured mobilities in discotics of the type HPAT₂ which become glasses at low T , over a wide range of temperatures. Here the mobility is strongly T dependent at low T .

Finally, the authors in Ref. 2 have shown that electrons and holes in HAT5 have very different mobilities: the hole mobility agrees with Fig. 7 and the electronic mobility measured by Adam *et al.*³ is activated with $E_a \sim 0.6$ eV. This difference we believe is due to the fact that electrons are in antibonding states and see a relatively small polarization barrier which can be surmounted thermally, but the coupling to the neutral neighbor is weak. A hole however sees a strong long range Coulomb field into which a negative charge can tunnel. The tunneling electron cannot thermally surmount the Coulomb potential, but it can find an efficient fluctuation assisted tunneling path over the 3.5 Å or so to the next core.

F. Origin of deep traps

Deep traps for holes can arise basically either because we have some hole (impurity or boundary) traps in the material, or there are structural defects which give rise to long hopping times, or we have double injection and holes are trapped by electrons that are also injected from the other electrode. Since in general the D phase has good transits and the C phase has not, we conclude that the change can be due to either of two effects; we assume that either (I) in the D_h phase we have fewer chemical deep traps or (II) the D_h phase has self-repairing structural properties and optimum wetting contact to the electrodes. Note: the electrode surfaces are not necessarily perfectly flat and this can give rise to strong misalignment effects in the crystalline phase.

It is unlikely that the D_h phase has substantially fewer hole scavengers than the C phase. Argument (II) however makes good sense; polycrystallinity is present and can be

TABLE I. Weak dispersion–linear response.

Dimensionality	Bias strength	Photocurrent decay
(a) $d=1$	$\eta < x$ $\eta = \frac{eFa}{2kT}$ $x = \text{trap concentration}$	$I_p(t)_{t \rightarrow \infty} \sim e^{-3[(\pi^2 x^2 t / 4a^2) D]^{1/3}}$ (exact analytic)
(b) $d=1$	$n > x$	$I_p(t)_{t \rightarrow \infty} \sim e^{-2\eta D_1 / a^2 t}$ (exact analytic)
(c) $d=3$	$\eta < x$	$I_p(t)_{t \rightarrow \infty} \sim e^{-[xt\sqrt{D_\perp D_\parallel}] / (a_\perp^2 + a_\parallel^2)}$ (first passage time)
(d) $d=1 \rightarrow 3$	$\eta < x$	$t \leq W_\perp^{-1}$ as in (a) $t \gg W_\perp^{-1}$ as in (c)
Diffusion		
Doped:		$\left \begin{array}{l} D(t) = D_0(T) + D_1 \left(\frac{t_0}{t} \right)^s, \quad s \sim 0.8, \quad \infty > t > t_0 \\ D_0(T) = D_c e^{-(T_0/T)^\gamma}, \quad s \sim \text{const}, \quad 0 < \gamma < 1 \end{array} \right $
low T diffusivity behavior due to barrier fluctuations		
Undoped:		$\left \begin{array}{l} D(t) = D_u(T) + D_\mu^{(1)} \left[\frac{t_0}{t} \right]^\alpha \\ D_u(t) = D_c e^{-(T_0/T)^2}, \quad 0 < \beta < 1, \quad T_0 = \sigma \end{array} \right $
$D(T)$ due to Gaussian fluctuations of polarization energy.		

seen by comparing the optical transmissivity of the two phases. We can conclude that the dispersion in C phases is mainly a result of grain boundaries and alignment. Holes injected in the C phase thermalize into the valence band tail where they encounter a distribution of deep structural traps. The spread in release times gives rise to Eq. (14) and also to dispersive transport. When the system enters the D phase, these traps appear and disappear in time on a rapid time scale; indeed the collective molecular motion associated with this dynamic ejects the particle back into the transport channel on the time scale of a microsecond or less and this self-averages the trap and release process giving us approximately what appears to be a slow but uniform charge motion. Each carrier then experiences, on average, the same trajectory despite the many scattering processes and delays encountered on the way. The trapping process can be expressed as an additional term in the stochastic self-energy as shown in Eq. (10). This term arises as a result of carriers being caught and released by rigidly displaced molecules from neighboring columns. If the release times are longer than the transit time as is the case in the C phase, the structural traps are effectively deep traps.

V. SUMMARY AND CONCLUSIONS

(i) We have presented a rigorous set of formulas to try to describe the photocurrent and photocurrent transits in columnar discotic liquid crystal.

(ii) We have shown that the degree of disorder can be characterized empirically and theoretically by a dispersion

parameter α . This is shown in Eq. (28) and this parameter can in turn be related to the distribution of jump rates $P(W)$ or trap rates. We have considered a variety of different scenarios, but on their own, none of the limits considered actually can be said to exactly describe the real situation. There are a number of reasons why this is so and these will become clear as we conclude (see Table I).

(iii) The long time photocurrent decays very slowly; it appears to reach a steady state at long times in the C phase. This suggests trap release and needs special theoretical treatment in 1D. This will be discussed elsewhere.

(iv) As it turns out, we are effectively always in the drift limited regime of decays so that appropriate simple exponential laws [Eq. (B3) in Appendix B] essentially suffice to fit the data and we have not been able to verify, in these experimental ranges, the subtle crossover between the diffusion and the drift limited decay regime predicted by exact theory for one-dimensional transport.

(v) Though dispersion must exist even in the liquid crystal phase, i.e., the transport along the columns is hindered by scattering from dynamical structural obstructions, the time scale of the frequency dependence or the scale of the dispersive region is short compared to our present experimental time so that, in the transit experiment, the drift appears to be perfectly regular except near the boundary at arrival. Here there appear to be traps, possibly injected space charge, which give a longer decay than diffusion theory (22) predicts. Again this needs special treatment.

(vi) We have been able to extract the trap density which immobilizes the carriers at least on a 10 μs time scale and is

characterized by a concentration “ x .” In order to compare with exact results on trapping kinetics these traps have been assumed to have no release time on the time scale of the experiment. We have therefore not distinguished between deep traps and recombination centers in this paper. Experiment however shows that not all traps are scavengers; some carriers can escape. This is clearly a reasonable scenario but needs a special mathematical treatment. The concentration of structural traps can be extracted by comparing the photocurrent decay in the C crystalline and liquid crystalline D phases; we found $x \sim 10^{-3}$.

(vii) Dimensionality crossover from 1D to 3D motion should occur on a time scale of an intercolumnar hop, which is roughly 10^3 to 10^6 times longer than an intracolumnar jump time.³⁰ This implies a time of order 10^{-6} s and therefore shorter than the actual transit time measured in Fig. 6. We could however not convincingly demonstrate crossover effects; see Figs. 2 and 4.

(viii) Motion in more than 1D manifests itself by a faster than “ $t^{1/3}$ ” law in the long time limit in small fields, but it also has a weakly field dependent trapping rate.²³ We have been able to fit these faster decay laws using a stretched exponential with an empirical parameter “ $\gamma \sim 0.65$ ”; no special significance could however be assigned to these fits since the corresponding parameters do not agree with those of the FPT theory which would exactly predict such a law.

(ix) We have shown that 1D motion cannot be deduced from the Gaussian transit behavior itself because the dimensionality can only manifest itself when “something unusual happens,” i.e., when there is deviation from perfect stochastic motion.

(x) Finally, we have shown how one could extract a “mobility order parameter” using rigorous transport theory and the data by Adam *et al.*²

Main conclusions for future work. The differences in the 1D to 3D kinetics appear in the following. (a) The trap controlled photocurrent decay and field dependence. This includes the shape of the photocurrent decay in transit experiments when there is a critical concentration of traps. It is therefore ironically the C phase which provides proof of 1D behavior. This is shown convincingly in Fig. 4. Future work will need to examine the diffusion region when $\eta < x$. (b) One-dimensional shallow trap limited mobility is known to have an anomalous electric-field dependence²¹ as long as the drift still depends on time; steady state drift is again normal and obeys linear response at small fields. These predictions may be verifiable in short glassy columnar materials; carriers stay on and around the same column on the experimental time scale while being “dragged” into barriers and traps by the field and one should initially observe sublinear drift velocities with field. This interesting effect needs to be investigated in detail in a future paper.

In this paper we have examined the photocurrent assuming normal linear response mobility; that is, we have considered case (a) or case (b) in the steady state. Anomalous transits need short pulses or ultrathin discotic films, and will, we hope, be studied in a future publication.

ACKNOWLEDGMENT

One of the authors, B.M., would like to thank the Leverhulme Trust for support.

APPENDIX A

The waiting time function can be simply estimated assuming (a) the traps are spatially distributed with $W = \nu \exp[-2\alpha R_{ij}]$, and a maximum accessible number N_t , or (b) the trap is spatial as above but release needs activation over an energy barrier E_t with a constant distribution $n(E_t) = 1/B$. We obtain, after a simple integral, the following.

Case (a):

$$\Psi(p) = 4\pi\alpha^{-d}N_t\{\ln[\nu/(p+p_0)]\}^d, \quad (\text{A1})$$

where d is the dimensionality of the distribution, and p_0 fixes the maximum number of lattice points on which the particle can reside in each transport site. For example, it means that if there is 1 extra site, then the dc diffusivity is reduced by a factor of (1/4), etc.

Case (b): fix distance to R_c for simplicity and vary the energy of the trap,

$$\Psi(p) = [kT/B](\nu/p)\ln\{[1 + p/\nu \exp(2\alpha R_c + B/kT)]/[1 + p/\nu \exp(2\alpha R_c)]\}; \quad (\text{A2})$$

assuming a scaling form, we can write $\Psi(p) = N_t(1/[(p/\nu_e)^\kappa + 1])$, where ν_e is a frequency which characterizes the delay process and κ is an exponent which characterizes the waiting time distribution. This is the form used to calculate Fig. 2.

APPENDIX B

Survival fraction in 1D in the regime of strong bias, i.e., $eFa/kT > x$ (trap density)

$$n(t) = n_1(t) + L(t), \quad (\text{B1})$$

where $n_1(t)$ is still given by Eq. (21) and now the new term L can be written

$$L(t) = \left\{ [8x^2(\eta-x)^2 \exp[-\eta^2 Dt/a^2]] \sum_0^\infty (n+1/2) \exp[Dt/a^2\{(\eta-x)/(2n+1)\}^2] / \{(2n\eta+x)(2n\eta+2\eta-x)\}^2 \right\}. \quad (\text{B2})$$

The reader should consult Refs. 16 and 17 for the asymptotic behavior of these functions. In the limit $\eta \gg x$, and $x \ll 1$, the $n=0$ term in the sum dominates and we have a simple exponential law

$$n(t) \sim \{4(\eta - x)^2 / (2\eta - x)^2\} \exp[-xv_d t], \quad \text{where } v_d = 2\eta D / kT. \quad (\text{B3})$$

-
- ¹S. Chandrasekhar and G. S. Raganath, Rep. Prog. Phys. **53**, 57 (1990).
- ²N. Boden, R. I. Bushby, J. Clements, M. Jesudason, P. Knowles, and G. Williams, Chem. Phys. Lett. **152**, 94 (1988).
- ³(a) D. Adam, F. Closs, T. Frey, D. Funhoff, D. Haarer, H. Ringsdorf, P. Schumacher, and S. K. Siemensmeyer, Phys. Rev. Lett. **70**, 457 (1993); (b) D. Adam, P. Schumacher, J. Simmerer, K. H. Eitzbach, H. Ringsdorf, and D. Haarer, Nature (London) **371**, 141 (1994); (c) H. Bengs, F. Closs, T. Frey, D. Funhoff, H. Ringsdorf, and K. Siemensmeyer, Liq. Cryst. **15**, 565 (1993).
- ⁴J. Clements, R. Bushby, B. Movaghar, N. Boden, K. Donovan, and T. Kreouzis, Phys. Rev. B **52**, 13 274 (1995).
- ⁵N. Boden, R. J. Bushby, and J. Clements, J. Chem. Phys. **98**, 5920 (1993).
- ⁶R. Y. Dong, D. Goldfarb, M. E. Moseley, Z. Luz, and H. Zimmermann, J. Phys. Chem. **88**, 3148 (1984).
- ⁷D. Markovitsi, I. Lecuyer, P. Lianos, and J. Malthete, J. Chem. Soc., Faraday Trans. **87**, 1785 (1991).
- ⁸D. Haarer and F. Moehwald, Phys. Rev. Lett. **34**, 1447 (1975).
- ⁹I. Hunt, D. Bloor, and B. Movaghar, J. Phys. C **16**, L623 (1983).
- ¹⁰U. Seiferheld, H. Baessler, and B. Movaghar, Phys. Rev. Lett. **48**, 532 (1982).
- ¹¹D. Dlott, M. D. Fayer, and R. D. Wieting, J. Chem. Phys. **69**, 2752 (1978), and references therein.
- ¹²S. Rughoputh, D. Bloor, D. Phillips, and B. Movaghar, Phys. Rev. B **35**, 8103 (1987).
- ¹³D. Adam, P. Schumacher, J. Simmerer, K. H. Eitzbach, H. Ringsdorf, and D. Haarer, Nature (London) **371**, 141 (1994).
- ¹⁴P. Allen, J. Phys. C **13**, L667 (1980).
- ¹⁵K. Arikainien, N. Boden, R. Bushby, J. Clements, and B. Movaghar, J. Chem. Phys. **5**, 2161 (1995).
- ¹⁶S. Alexander, J. Bernasconi, R. Orbach, and W. R. Schneider, Rev. Mod. Phys. **53**, 175 (1981).
- ¹⁷B. Movaghar, D. Wurtz, and B. Pohlmann, Z. Phys. B **66**, 523 (1987).
- ¹⁸H. Scher and M. Lax, Phys. Rev. B **7**, 4491 (1973).
- ¹⁹D. Adam, W. Rohmildt, and D. Haarer, *Proceedings of the Japan "Liquid Crystals" Workshop: "Metallomesogens and Discotic Liquid Crystals"* (ONRI, Osaka, Japan, 1995), p. 100.
- ²⁰S. Chandrasekhar, *Liquid Crystals*, Cambridge Monographs on Physics (Cambridge University Press, Cambridge, UK, 1980).
- ²¹(a) B. Movaghar and W. Schirmacher, J. Phys. C **14**, 859 (1981); (b) B. Movaghar, B. Pohlmann, D. Wurtz, M. Gruenewald, and W. Schirmacher, J. Stat. Phys. **30**, 315 (1983).
- ²²B. Movaghar, D. W. Murray, K. J. Donovan, and E. G. Wilson, J. Phys. C **17**, 1247 (1984).
- ²³B. Movaghar, Semicond. Sci. Technol. **4**, 95 (1989).
- ²⁴B. Movaghar, B. Pohlman, and D. Wurtz, Phys. Rev. A **29**, 1568 (1984).
- ²⁵T. Phillips and J. C. Jones, Liq. Cryst. **16**, 805 (1994).
- ²⁶B. Movaghar, B. P. Pohlmann, and D. Wurtz, in *Polydiacetylenes*, Vol. 102 of *NATO Advanced Study Institute, Series E: Applied Sciences*, edited by D. Bloor and R. Chance (Martinus Nijhoff, Dordrecht, 1985), p. 177.
- ²⁷H. Scher and E. W. Montroll, Phys. Rev. B **12**, 2455 (1975).
- ²⁸M. Funahashi and Jun-ichi Hanna, Phys. Rev. Lett. **78**, 2184 (1997).
- ²⁹B. Movaghar and J. Leo, Phys. Rev. B **38**, 8061 (1988).
- ³⁰J. Warman, M. P. de Haas, K. I. Smit, M. N. Paddon-Row, and J. F. van der Pol, Mol. Cryst. Liq. Cryst. **183**, 375 (1990).